This is the Pre-Published Version.
R. Bu, Y. Zhou, X. Huang, C. Fan (2023) *Flame spread over convex and inclined flat surfaces*, **Fire Safety Journal** ,103955.
(SI of 14th IAFSS Symposium) https://doi.org/10.1016/j.firesaf.2023.103955

Flame Spread over Convex and Inclined Flat Surfaces

Rongwei Bu[a,b], Yang Zhou[a,b*], Xinyan Huang[c*], Chuangang Fan[a,b]

[a]School of Civil Engineering, Central South University, Changsha, China,

[b]Hunan Provincial Key Laboratory for Disaster Prevention and Mitigation of Rail Transit Engineering Structures, Central South University, Changsha, China

[c]Department of Building Environment and Energy Engineering, The Hong Kong Polytechnic University, Hong Kong, China,

*Corresponding to zyzhou@csu.edu.cn, xy.huang@polyu.edu.hk

Highlights

- Flame spread characteristics of convex surface were experimentally studied
- Horizontal flame spread rate of convex surface was close to that of flat surface
- Radiant heat flux received by sample rear was characterized by two peaks at $\varphi \geq 45^{\circ}$
- Compared to convex surface, the convection contribution was larger for flat surface

Abstract: Convex surface is a general configuration in various building structures. Most studies for flame spread only investigated the flat surface type, while the flame spread over convex surface has not been addressed yet. A comparative study of convex and inclined flat surfaces was therefore performed by designing different curvatures (reflected by central angle φ) and flat-slope inclination angles (denoted by θ). The thermally thin PMMA sheet with a fixed horizontal projection length of 500 mm was chosen. The average path flame spread rate presents an exponential growth with increasing φ and θ. Moreover, the average horizontal flame spread rates of convex and inclined flat surfaces are close. For convex surface, radiant heat flux received by the sample rear increases with increasing φ. Also, two peaks of radiant heat flux occur at $\varphi \geq 45^{\circ}$. However, convective heat flux increases suddenly when $\theta \geq 22.5^{\circ}$, in which convective heat transfer was the main mechanism. In addition, with increasing φ and θ, overall burnout rate increases for convex surface, but has an increasing first and then decreasing tendency for flat surface. It is found that the convection contribution on the pyrolysis zone is more obvious for inclined flat surface, in comparison to convex surface.

Keywords: flame spread; convex surface; curvature; radiant heat flux; overall burnout rate

1. Introduction

Flame spread is a fundamental problem of fire research. Characteristics of flame spread depend on the combustible configuration, such as fuel inclination angle [1,2], fuel dimension [3,4], fuel shape [5,6], etc. In terms of building fires, the influence of fuel shape is characterized by building structure form. For the purpose of aesthetic, the building façade is designed as various geometries. Flat shape [7], U-

shape [8], L-shape [9], and vertical channel [10], as common building structure forms, have been concerned well. Curved surface (e.g. convex surface) is also a typical form in building structures (see Fig. 1), such as curved exterior façade [7], curved sunshade [11], etc.

For curved surface, the inclination angle of fuel is significantly time-varying with the progression of the pyrolysis front. However, most studies on flame spread [1−4,7−10,12−18] only concern flat surface configuration. Moreover, to facilitate research, the surface configuration is also generally simplified as flat configuration even for complex surface configuration [7,12,23]. The difference in flame spread caused by different surface configurations (e.g. convex and flat surfaces) is not always known. Therefore, a preliminary understanding of the flame spread behavior of curved surface is necessary.

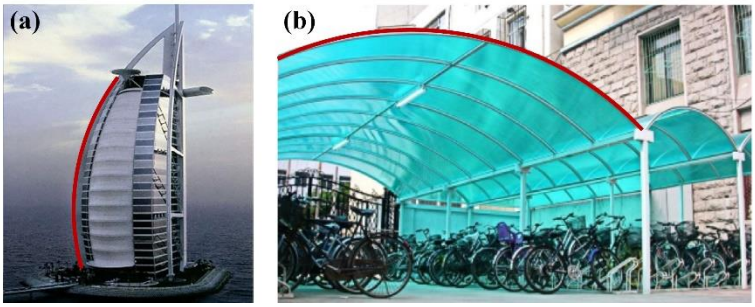

Fig. 1. Real scenarios of curved surface: (a) high-rise building façade [7]; (b) sun shade [11].

For flat surface, the influence of inclination angle on flame spread has been addressed well [1,2,7,14−18]. With increasing inclination angle, the component of buoyancy parallel to the fuel surface increases, and then flame regimes change from “pool fire” to “wall fire” [1,14,15]. Moreover, with the transition of flame regime, the heat transfer mechanism is converted from radiant dominance to convective dominance [2]. The controlled mechanism is related to the fuel dimension. For a large sample with 10 cm wide, mass loss rate per unit area decreases with increasing inclination angle [1], for which radiant heat transfer is responsible. However, Zhao et al. [15] found that mass loss rate per unit area increased along with a larger inclination angle for the sample with 5 cm wide. For a small sample, convective heating dominated burning. Width effect is contributed by heat loss and lateral fuel diffusion, and air entrainment [16]. Moreover, when sample width is larger than 10 cm, heat loss and lateral fuel diffusion become unimportant [16,17].

With the increase of inclination angle, the preheating zone length is extended, accelerating the flame spread rate (FSR). Drysdale and Macmillan [18] found that for thermally thick fuels, the acceleration of flame spread occurred at the angle of 15−20°. For thermally thin fuels, a sudden rise in FSR was experimentally determined at 10−20° [19], and the critical model of acceleration was established. Using a modified *B*-number, Pizzo et al. [20] developed a transient pyrolysis model, and found that the model could predict the FSR well above the critical angle, i.e. 20°. Moreover, based on the heat transfer analysis,

Huang et al. [2] and Zhou et al. [14] proposed the semi-empirical correlation of FSR in the inclined orientation. Qi et al. [21] and Zhou et al. [22] developed an empirical correlation of FSR.

Recently, Tao et al. [11] investigated the ignition risk of the cylindrical sample, and found that the risk of the cylindrical sample was higher than that of the slab sample. Sun et al. [23] studied the influence of flame spread paths on the overall flame spread rate, and explored the "brachistochrone path". It was found that the inclination angle, shape, and path height had an important effect on travel time. However, flame spread characteristics of curved surfaces are not addressed well.

This study provides new insight into how flame spreads along curved surface. Convex surface is selected as a representative curved surface herein. Classical flame spread parameters, including FSR, heat flux, mass loss rate (MLR), and burnout rate, are concerned. The results will bring a new understanding of flame spread over solid.

2. Experimental setup

Figure 2 shows the experimental apparatus for flame spread over convex and inclined flat surfaces. Side-view and front-view cameras (SONY, FDR-AX100E) were employed to record the flame spread process at 25 fps. Total and radiant heat fluxes were measured by the Schmidt-Boelter heat-flux gauge installed at the sample rear. The uncertainty is less than ±3%, and the sampling frequency is 10 Hz. Two K-type thermocouples with a 0.5 mm diameter were arranged on the sample surface and above the heat flux gauge to measure the characteristic temperature of gas phase. An electronic balance (Sartorius, PMA35001) with an accuracy of 0.1 g was placed on the bottom of the fireproof board to capture the mass variation at 5 Hz. Moreover, a dial scale was fixed in the holder to determine the scale ratio of flame images.

Polymethyl methacrylate (PMMA) with dimensions of 10 cm wide (W) and 3 mm thick (d) was selected as the sample. For all tested PMMA samples, the horizontal projection distance (l_r) is fixed to 0.5 m, which is the control parameter. The fixed horizontal projection distance of 0.5 m can ensure enough flame travel time (>10 min) to reduce the ignition effect, and is also available to compare the curvature effect. For convex surface, six kinds of central angles (φ, 15°, 30°, 45°, 60°, 75°, and 90°), were designed. Curvature was calculated by $\sin\varphi/l_r$, thus the angle φ was employed to reflect the influence of curvature in this study. Corresponding to the six curvatures, six kinds of inclined flat surfaces (θ, 7.5°, 15°, 22.5°, 30°, 37.5°, and 45°) with the same path height and horizontal projected length were also designed as the comparison conditions. In addition, zirconium fire blanket with the thermal conductivity of 0.09 W/(m·K) was placed between sample and holder to simulate the adiabatic boundary.

In this study, the largest Biot number, defined as $Bi = dh / k_s$ (thickness d was 3 mm, thermal conductivity k_s was 0.19 W/(m·K) [24], and maximum convective heat transfer coefficient h for convex and inclined flat surface [25,26] was calculated as 13.62 and 17.55 W/(m^2·K) respectively), were

calculated as 0.22 and 0.28 for convex and inclined flat surfaces, respectively. Therefore, the sample was approximated to be thermally thin. Sample width of 10 cm could also avoid the influence of lateral fuel diffusion [16]. Moreover, scale lines with 5 cm spacing were drawn on the fuel surface to determine the pyrolysis length and the progression of pyrolysis front position. Experimental designs of convex and inclined flat surfaces are listed in Table 1. Each condition was repeated 3−4 times to ensure repeatability.

Table 1 Experimental designs of flame spread over convex and inclined flat surfaces.

Condition	Convex surface			Flat surface
	Central angle (φ) / °	Curvature / m^{-1}	Equivalent radius / m	Inclination angle (θ) / °
1	15	0.52	1.9	7.5
2	30	1.0	1.0	15.0
3	45	1.4	0.71	22.5
4	60	1.7	0.58	30.0
5	75	1.9	0.52	37.5
6	90	2.0	0.5	45.0

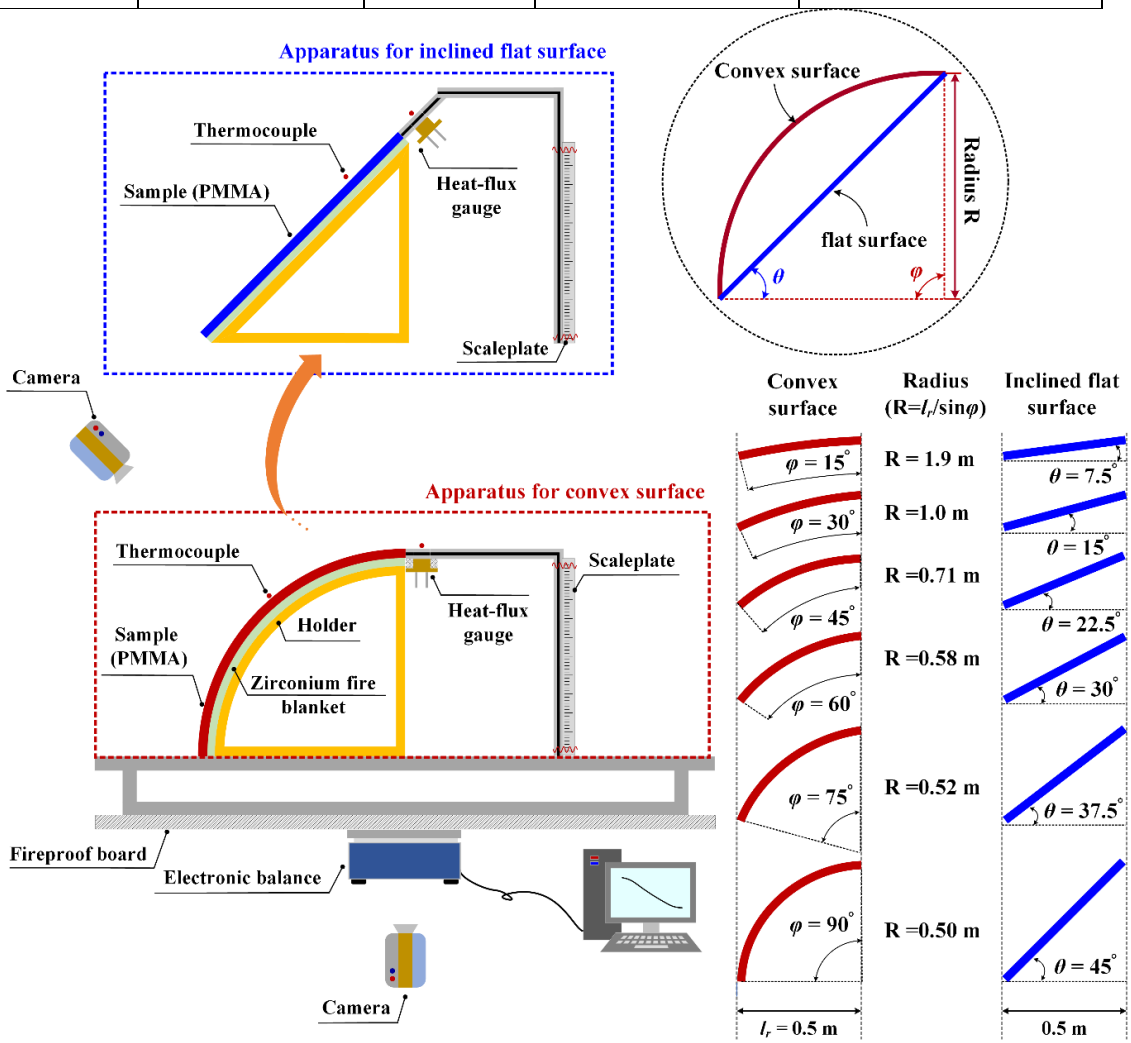

Fig. 2. Experimental apparatus for flame spread over convex and inclined flat surfaces.

3. Results and discussion

3.1 Physical observations

Figure 3 shows the development of flame shape along convex and inclined flat surfaces when $\varphi = 90^{\circ}$ and $\theta = 45^{\circ}$. For convex surface, the tangent angle at the pyrolysis front gradually decreases during the flame spread process, increasing the symmetry of air entrainment between two sides of flame surface. Therefore, flame configuration changes from wall-fire to pool fire regime with time. Moreover, pyrolysis length and flame length present an obvious time-varying process. Different from convex surface, flame attachment phenomenon is significant for inclined flat surface with $\theta = 45^{\circ}$.

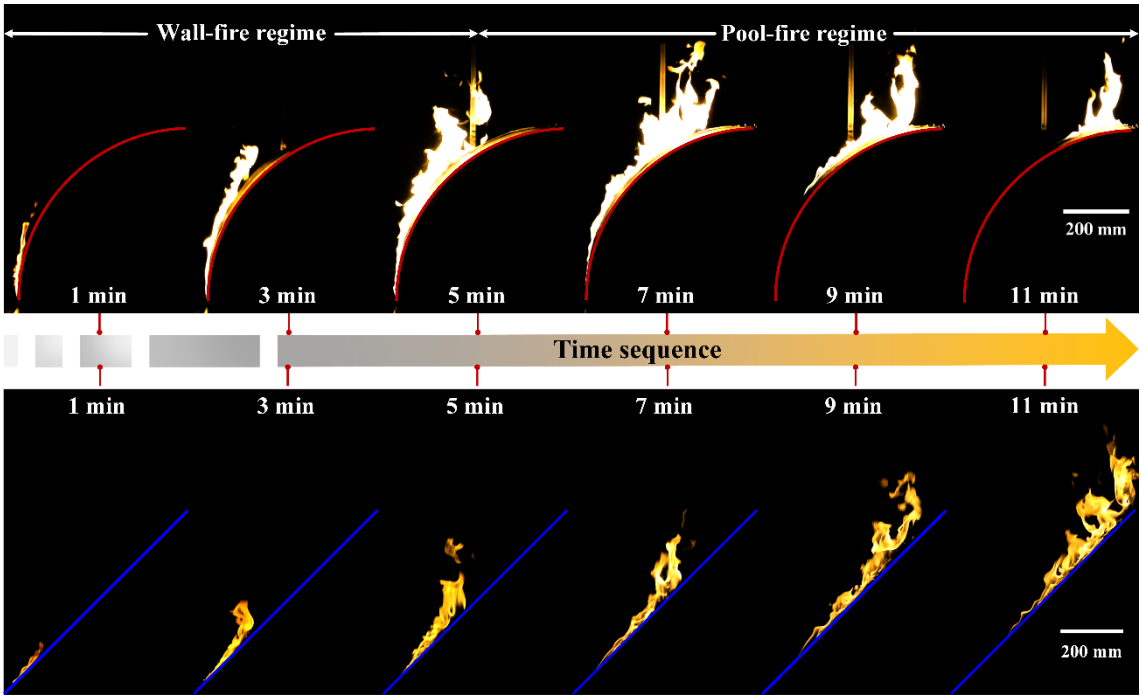

Fig. 3. Flame spread process of convex surface at φ = 90°and inclined flat surface at θ = 45°.

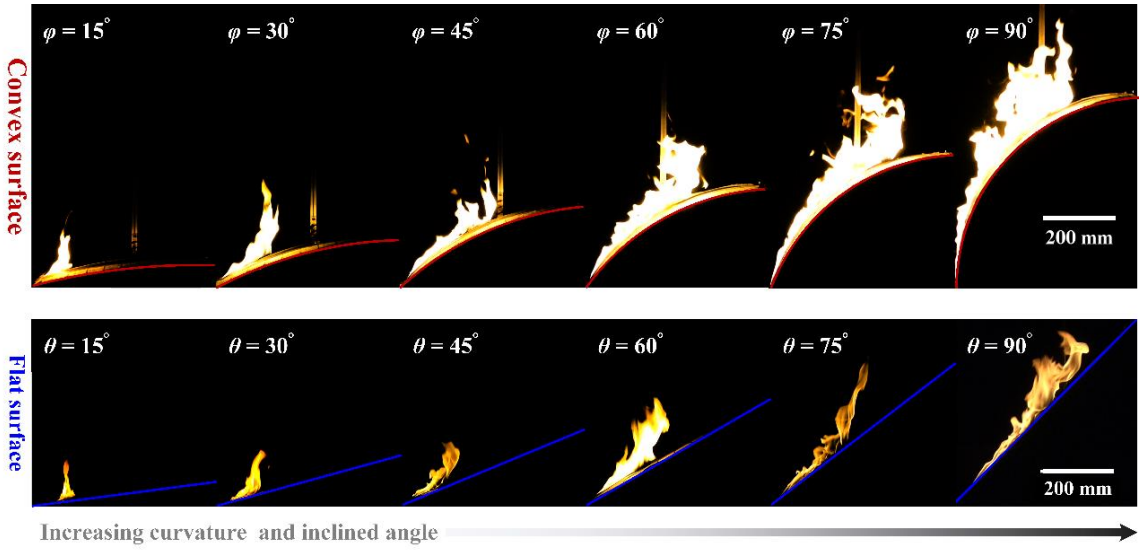

Fig. 4. The influence of surface shape on flame structure at t = 6 min.

The influences of curvature and inclination angle on flame structure are shown in Fig. 4. Similar to inclined flat surface, path flame spread rate (PFSR) and pyrolysis length increase along with a bigger curvature. For inclined flat surface, with an increasing inclination angle, the buoyancy component parallel to the fuel surface increases, increasing the pressure difference between the two sides of flame surface. Therefore, flame tilt angle gradually decreases, which is consistent with previous studies [15,22]. However, flame attachment phenomenon does not occur for convex surface when t = 6 min. In addition, compared to inclined flat surface, the flame thickness is larger for convex surface.

3.2 Path and horizontal flame spread rates

Under different curvatures and inclination angles, the progressions of pyrolysis front position x_p with time are plotted in Fig. 5. During the flame spread process of convex surface, PFSR has a slightly decreasing tendency with time, as shown in Fig. 5(a). For convex surface, the tangent angle of fuel surface decreases with the progression of the pyrolysis front. The restriction of air entrainment between flame surface and fuel surface decreases, lifting flame standoff distance. Therefore, the flame heat flux to preheating zone decreases. For flame spread over inclined flat surface, the acceleration of flame spread occurs at $\theta \geq 22.5^{\circ}$, as shown in Fig. 5 (b). It can be known from Fig. 3 that during the process, flame length and the preheating length increase, increasing the heat transfer from the flame to the preheating zone.

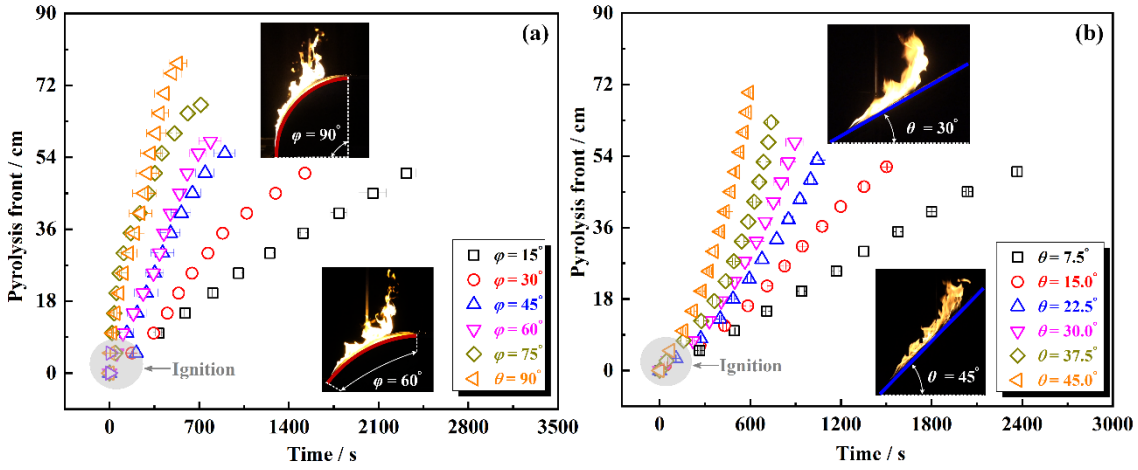

Fig. 5. The progression of pyrolysis front with time: (a) convex surface; (b) inclined flat surface.

To further evaluate the surface shape effect, the average PFSR is introduced, defined as $\overline{v_f} = \frac{1}{t}\int_0^t \frac{dx_p}{dt}dt$.

The dependencies of curvature and inclination angle on average PFSR are shown in Fig. 6, along with the comparison of previous studies [1,2,16,18,20]. It can be seen that the average PFSR increases along with a bigger curvature and inclination angle. With increasing curvature and inclination angle, the component of buoyancy flow along fuel surface increases, stretching the preheating length. Moreover, with increasing φ and θ, the air entrainment restriction near flame surface increases, pushing flame

surface closer to the fuel surface. Therefore, the heat transfer from the flame to the fuel surface is enhanced, increasing the average PFSR. In addition, PFSR is also sensitive to sample size. Under the influences of width, thickness, and edge effect, there are differences among previous studies for flat surface. Radiation and convection received by the preheating and pyrolysis zones are both influenced by sample width and thickness [27,28], and the thermal inertia of sample depends on sample thickness.

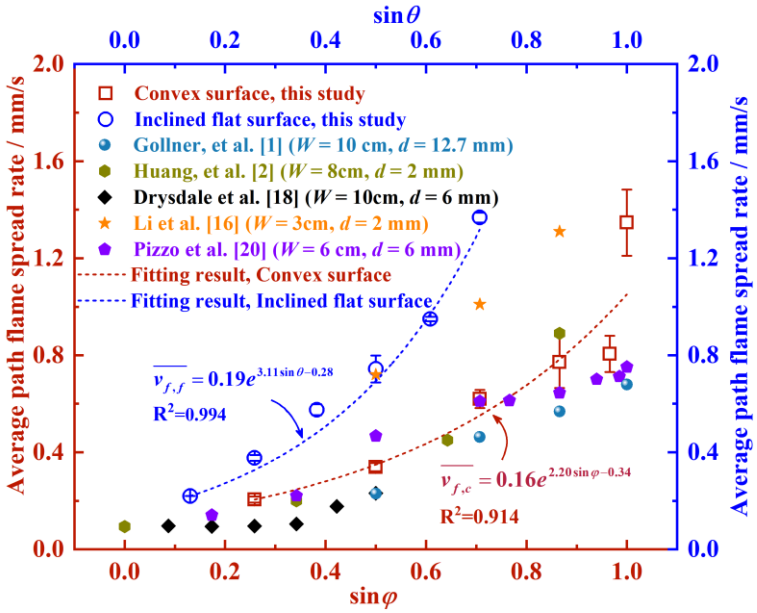

Fig. 6. The influences of curvature and inclination angle on average PFSR.

For inclined flat surface, the relationship between $\overline{v_f}$ and θ has been empirically quantified by exponential correlation. Qi et al. [21] proposed the exponential correlation between $\overline{v_f}$ and θ through flame spread experiments of log planks. Using rigid polyurethane foam, Zhou et al. [22] found that $\overline{v_f}$ was an obvious exponential function of sinθ. From Fig. 6, it can be seen that $\overline{v_f}$ has an exponential dependency on sinθ and sinφ for convex and inclined flat surfaces. The mathematical correlations of convex and inclined flat surfaces are summarized as follows:

$$\overline{v_{f,c}} = 0.16e^{2.20\sin\varphi-0.34}, \text{ for convex surface} \quad (1)$$

$$\overline{v_{f,f}} = 0.19e^{3.11\sin\theta-0.28}, \text{ for inclined flat surface} \quad (2)$$

where subscript c and f denote the convex and inclined flat surfaces, respectively. According to the expression of curvature (i.e. $\sin\varphi/l_r$), Equation (2) also reflects the correlation between average PFSR and curvature.

In addition to the PFSR, horizontal flame spread rate (HFSR) is also an important parameter to evaluate fire hazards for the different surface configurations with the same horizontal projection distance. HFSR $v_{f,h}$ is the horizontal component of PFSR. Similar to the average PFSR, the average HFSR is introduced,

$\overline{v_{f,\ h}} = \frac{1}{t}\int_0^t \frac{dx_{p,h}}{dt}dt$, where $x_{p,h}$ is the pyrolysis front position regarding the horizontal axis. It can be seen that $\overline{v_{f,h}}$ also increases along with a bigger curvature and inclination angle. However, within $45^\circ \le \varphi \le 75^\circ$, there is a wiggle in PFSR and HFSR as shown in Figs. 6 and 7. Under a large curvature, the transition from wall-fire to pool-fire regime is significant during the flame spread process. It may indicate the change in the heat transfer mechanism from convection to radiation dominance. The convective-dominated spread affects the large range, resulting in the wiggle effect.

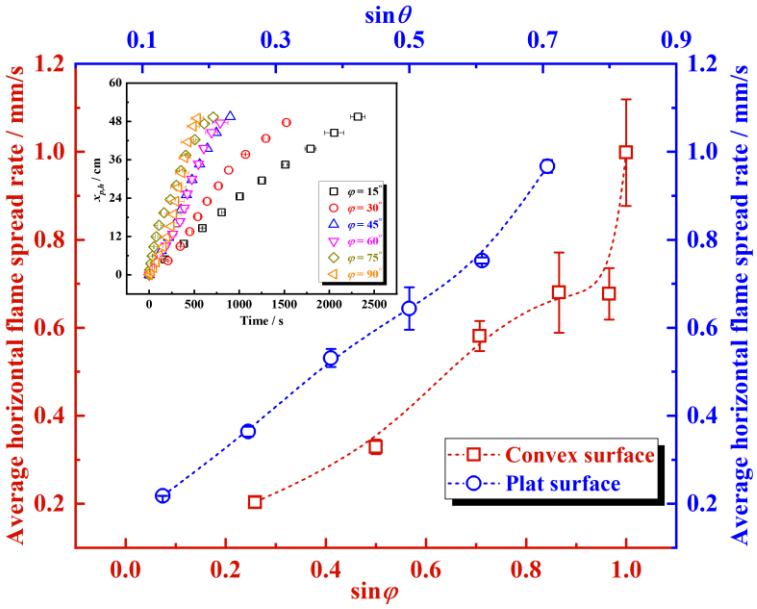

Fig. 7. Average HFSRs under different curvatures and inclination angles.

To further compare the difference between convex and inclined flat surfaces, dimensionless HFSR v_f^* and structure factor ϕ are introduced. Dimensionless HFSR is defined as the ratio of average HFSR of convex surface $\overline{v_{f,c-h}}$ to that of inclined flat surface $\overline{v_{f,f-h}}$, and the structure factor ϕ is expressed as the ratio of path height (H) to l_r. The relationship between v_f^* and ϕ is plotted as shown in Fig. 8. Under different structure factors, v_f^* is approximately constant, $v_f^* \approx 0.99$. Although the flame travel paths are different for convex and inclined flat surfaces, the horizontal flame spread rates are close. The correlation between $\overline{v_{f,c}}$ and $\overline{v_{f,h}}$ can be approximately deduced as follows:

$$\frac{\overline{v_{f,c-h}}}{\overline{v_{f,f-h}}} = \frac{(1/(\varphi R))\int_0^{\varphi R} v_{f,c}\cos(\varphi - x_p/R)dx_p}{\overline{v_{f,f}}\cos\theta} \approx \frac{\overline{v_{f,c}}\sin\varphi}{\overline{v_{f,f}}\varphi\cos\theta} \qquad (3)$$

Here, based on the assumption of constant v_f^*, the relationship between $\overline{v_{f,c}}$ and $\overline{v_{f,h}}$ can be further written as:

$$\overline{v_{f,c}} \approx 0.99\overline{v_{f,f}}\,\varphi\cos\theta/\sin\varphi \qquad (4)$$

It reflects the connection between convex and flat surfaces, and provides a simple method to evaluate the PFSR of curved surface.

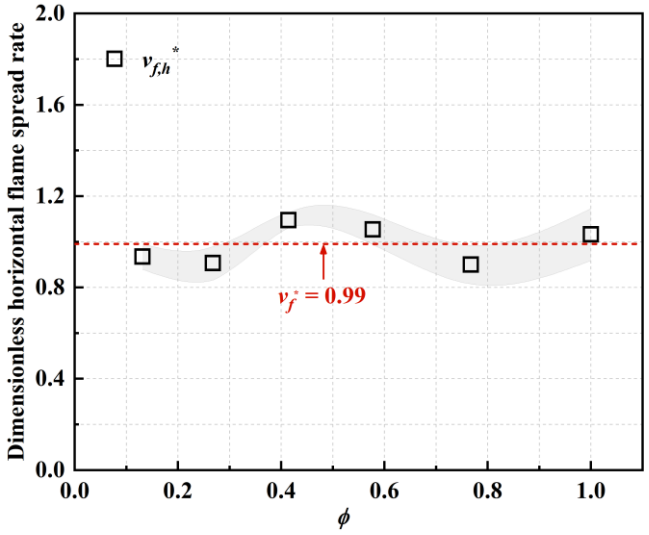

Fig. 8. Relationship between dimensionless HFSR and structure factor.

3.3 Radiant heat transfer

Heat-flux gauge was arranged 40 mm away from the sample rear. The progressions of heat fluxes are plotted in Fig. 9 both for convex and inclined flat surfaces. For convex surface, radiant and total heat fluxes increase along with a bigger φ. Moreover, when $\varphi \geq 45^\circ$, two peaks of radiant heat flux occur, as shown in Fig. 8 (a). Radiant heat flux received by the unburned zone depends on view factor and flame emissivity. The view factor is related to the area of flame surface, and flame emissivity is sensitive to the characteristic length of burning zone l_c. By assuming the pyrolysis zone as circular pool fire geometry [27], l_c can be expressed as $l_c = \sqrt{4A/\pi}$, where l_p is the pyrolysis length and the pyrolysis area A is approximated as $A = l_p W/2$. As shown in Figs. 3 and 10, flame length and characteristic length increase first and then decrease during the spread stage. The maximum flame length and characteristic length lead to the first peak. As the pyrolysis front reaches the sample rear, the second peak is achieved. During the flame spread stage, radiant heat transfer is the main mechanism for the heating of the sample rear. Moreover, the characteristic length l_c is positively related to sample width and thickness. It can be inferred that with the increase of sample width and thickness, the feature of two peaks will become more obvious.

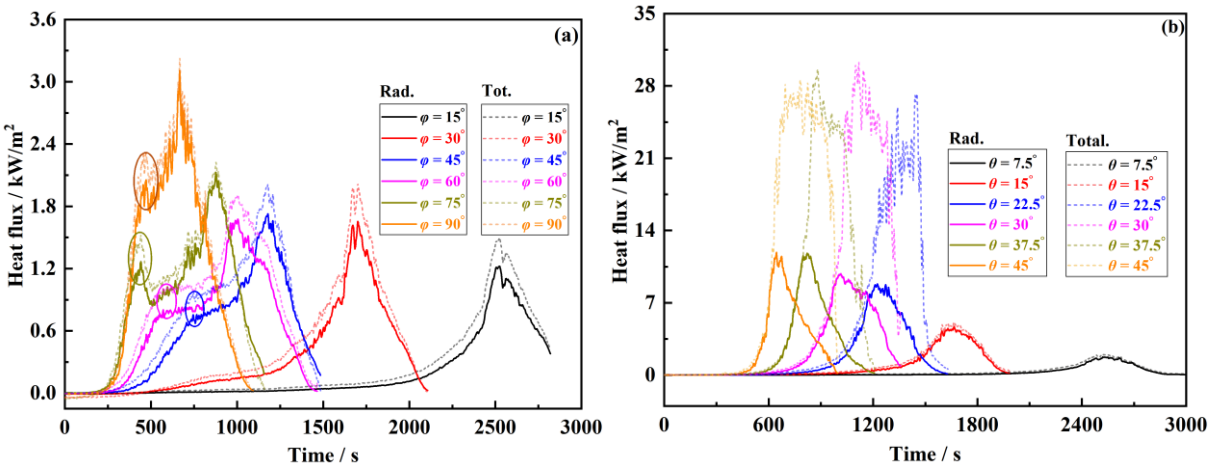

Fig. 9. The evolution of the measured heat flux with time: (a) convex surface; (b) inclined flat surface.

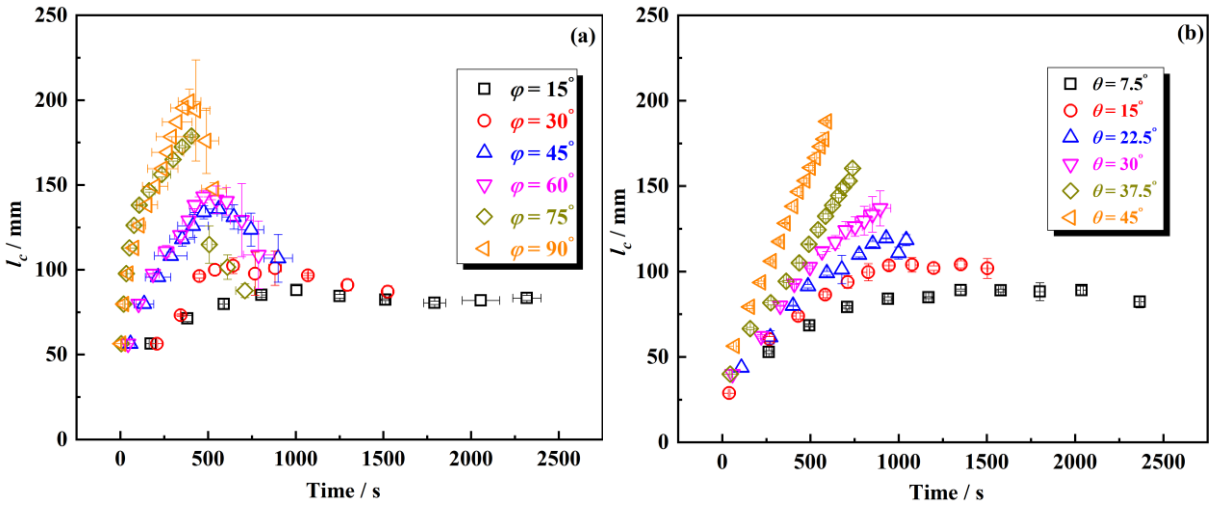

Fig. 10. The progression of characteristic length with time: (a) convex surface; (b) inclined flat surface.

Similar to convex surface, radiant and total heat fluxes also increase with increasing θ. Moreover, when $\theta \geq 22.5^{\circ}$, total heat flux sharply increases, and is greater than radiant heat flux. It indicates that with increasing θ, the heat transfer mechanism is changed from radiation dominance to convection dominance, which is consistent with previous studies [2,14]. The main reason is that as θ increases, flame tilt angle decreases rapidly under the Coanda effect. Here, when $\theta \geq 22.5^{\circ}$, the heat transfer mechanism changes for inclined flat surface, corresponding to the occurrence of two peaks for convex surface with $\varphi \geq 45^{\circ}$.

3.4 Mass loss rate and overall burnout rate

During the flame spread stage, the evolutions of MLR are plotted in Fig. 11. For convex surface, MLR increases first and then decreases with time. However, when $\theta \geq 22.5^{\circ}$, MLR presents an increasing tendency with time for inclined flat surface. MLR is dependent on the characteristic length of pyrolysis zone and flame heat flux. As shown in Figs. 10 and 11, the variation of MLR is the same as the characteristic length l_c.

For thermally thin materials, in-depth absorption is unimportant due to the uniform temperature distribution within the solid phase. Therefore, the energy balance in the pyrolysis zone is

$$\dot{m}'' \sim \dot{q}''_{f,r} + \dot{q}''_{f,c} - \dot{q}''_{s,c} - \dot{q}''_{s,r} \qquad (5)$$

where $\dot{q}''_{f,r}$ is radiant heat transfer from the flame to the burning zone; $\dot{q}''_{f,r}$ is convective heat flux received by the burning zone; $\dot{q}''_{s,c}$ is the thermal conduction of solid phase, and can be neglected for the thermally thin fuels; $\dot{q}''_{s,r}$ is re-radiation heat flux, which can be assumed to be constant. $\dot{q}''_{f,c}$ is the function of l_c [27], and is approximated as $\dot{q}''_{f,r} \propto l_c$ by assuming that the view factor and flame temperature are insensitive to l_c. During the flame spread process, the ranges of Rayleigh number of pyrolysis zones for convex and flat surfaces are 1.2×10^5–3.4×10^6 and 8.7×10^4–9.1×10^7 respectively, which are both in the laminar regime. Therefore, according to the convection heat transfer correlations of curved surface [25] and inclined plate [26], $\dot{q}''_{f,c}$ can be expressed as $\dot{q}''_{f,c} \propto l_c^{-1/4}$. Therefore, MLR is an obvious function of l_c, $\dot{m} = f(l_c)$. It should be noted that the heat input from the flame to the pyrolysis zone is also weakened by the heat blockage effect caused by the fuel vapors, soot, and products of combustion near the burning fuel surface. However, the blockage factor is found to be almost constant [29]. In other words, although heat transfer models overestimate the heat input, the qualitative variation tendency can be still reflected.

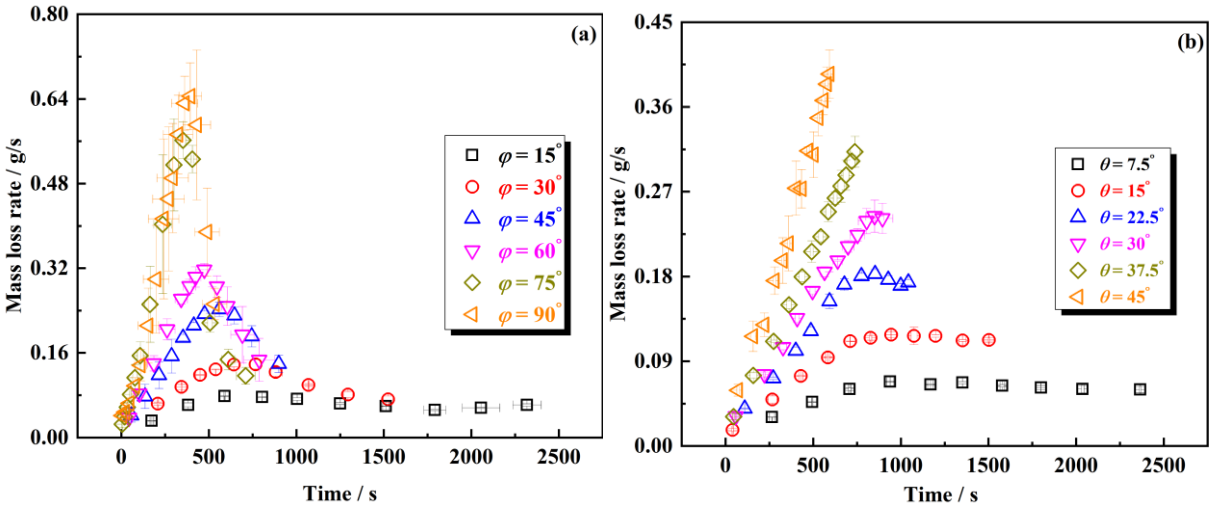

Fig. 11. The progression of mass loss rate with time: (a) convex surface; (b) inclined flat surface.

According to Eq. (4), MLR under different dominance mechanisms can be simply described as: $\dot{m} \propto l_c^{3.0}$, for radiant dominance; $\dot{m} \propto l_c^{7/4}$ for convection dominance. For laminar convective burning on vertical surface [30], local mass loss rate per unit area is a function of the location of the pyrolysis zone, $\dot{m}''_x \propto x^{-1/4}$. Therefore, under convective dominance, MLR can be written as:

$\dot{m} = \int_0^{l_p} \dot{m}'' dx = W \int_0^{l_p} \dot{m}' dx \propto l_p^{3/4} \propto l_c^{3/2}$. Under convective dominance, the difference in power index is caused by the difference between average and local convective heat transfer.

The relationship between $\dot{m}$ and l_c are plotted in Fig. 12. MLR has an obvious power-law dependency on l_c. For convex surface, the power index is found to be 2.30. It indicates that the burning of pyrolysis zone is dominated by the combined effect of radiant and convective heat transfer. For inclined flat surface, $\dot{m}$ at $\theta \geq 22.5^\circ$ is larger than that at $\theta < 22.5^\circ$ under a fixed l_c. The main reason is that for a larger θ, the burning area is large. Besides, due to the flame attachment, the boundary layer thickness is decreased at a large θ, increasing the local convective heating rate. Moreover, for inclined flat surface, the power index is low and close to 7/4. Therefore, the burning is controlled by convection heat transfer. Huang et al. [2] also found that in the inclined configuration, convective heat transfer dominated the burning in most cases. Therefore, during the flame spread stage, the contribution of convective heat transfer on burning is more important for inclined flat surface, in comparison to convex surface.

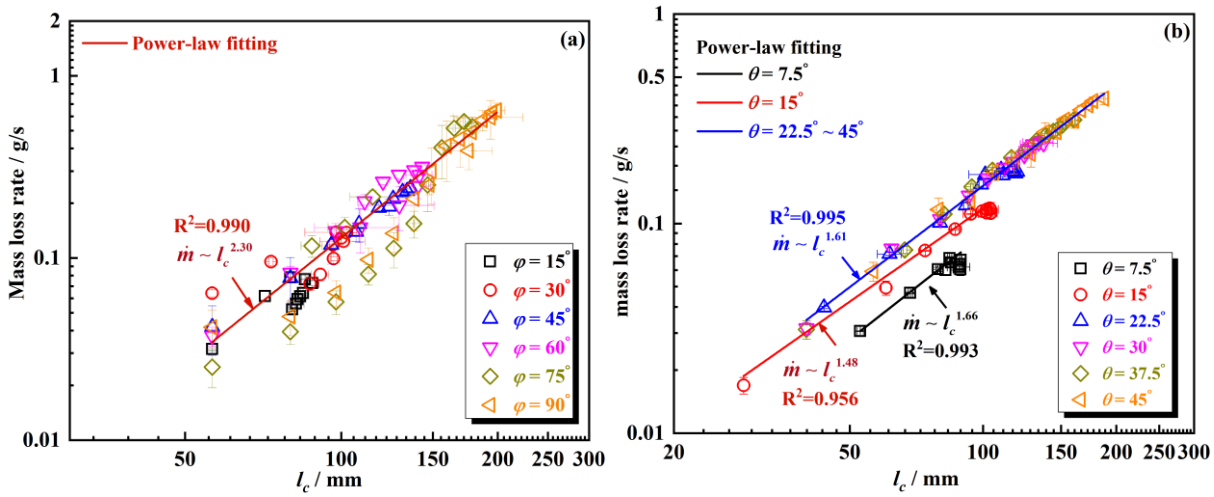

Fig. 12. Mass loss rate vs. characteristic length: (a) convex surface; (b) inclined flat surface.

From Figs. 3 and 10, burnout effect runs through the flame spread process. Burnout effect is a joint result of material property, local heat transfer, and the length of pyrolysis zone, and determines the establishment of steady state [18]. The evolutions of burnout front with time are shown in Fig. 13. Under a large curvature, the inclination angle at the rear of pyrolysis zone is large, resulting in large local convective heating. However, from Fig. 3 (a), the burnout front remains unchanged at the initial stage (< 450 s) for $\varphi = 90^\circ$, which may indicate the importance of radiant heat transfer on burnout effect. After that, burnout front rapidly increases due to rapid decrease of pyrolysis length as shown in Fig. 10.

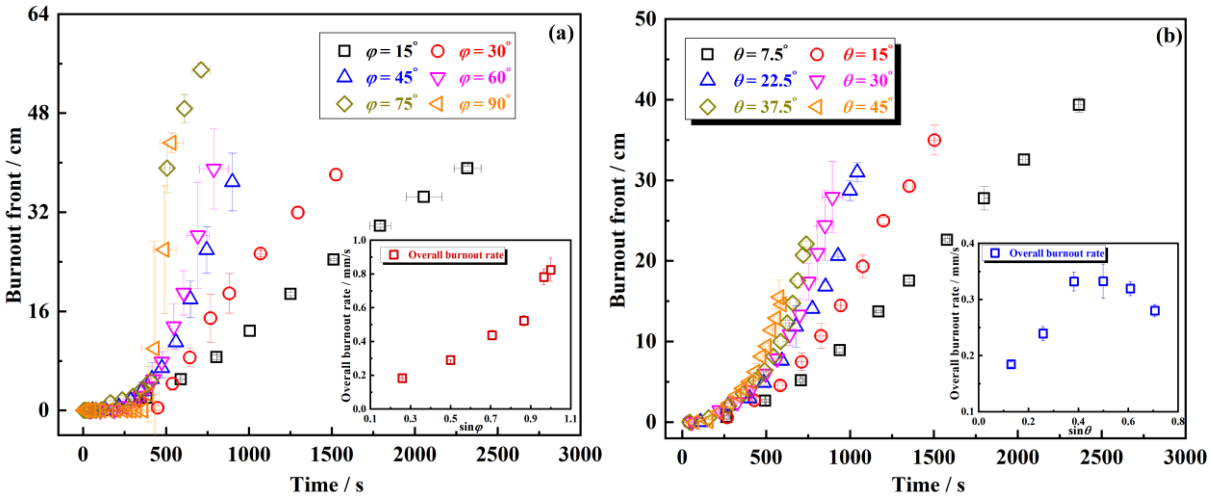

Fig. 13. The progression of burnout front with time: (a) convex surface; (b) inclined flat surface.

To evaluate the burnout effect, the overall burnout rate, defined as the ratio of the overall burnout distance to overall burnout time, is introduced. From Figs. 9 and 13, for convex surface, radiant heat transfer increases with increasing φ, resulting in the increase of overall burnout rate. For inclined flat surface, as θ increases, the overall burnout rate presents an increasing first and then decreasing tendency, which is caused by the transition of radiation to convection dominance. In addition, the overall burnout rate of convex surface is higher than that of inclined flat surface. It indicates that compared to the inclined flat surface, the radiant heat transfer is more important for convex surface, which is consistent with the results of Fig. 12.

4. Conclusions

In this study, the influence of surface shape on flame spread characteristics was investigated by fire tests on thin PMMA samples under different curvatures and inclination angles. The main conclusions are as follows:

(1) For convex and inclined flat surfaces, the average PFSR increases along with a larger curvature and inclination angle, and can be described by exponential correlations well. Moreover, it is found that the ratio of the average HFSR of convex surface to that of inclined flat surface is approximately constant.

(2) Radiant heat flux received by the sample rear increases with increasing curvature and inclination angle. When $\varphi \geq 45^{\circ}$, two peaks of radiant heat flux occur for convex surface. When $\theta \geq 22.5^{\circ}$, convective heat flux is the main heat transfer mechanism due to the flame attachment for inclined flat surface.

(3) With increasing θ and φ, the overall burnout rate increases for convex surface, but has an increasing first and then decreasing tendency for inclined flat surface. Also, compared to convex surface, the convective heating effect on the burning zone is more obvious for inclined flat surface.

This study serves as a preliminary step of determining flame spread characteristics of curved surface, and has also limitations. For example, sample size together with the more complex curved surface is not addressed in this work, which will be concerned in our future work.

Acknowledgments

This work is supported by the National Natural Science Foundation of China (No. 52278545), Natural Science Foundation of Hunan Province (No. 2021JJ30860), Central South University Research Programme of Advanced Interdisciplinary Studies (No. 2023QYJC024), and Fundamental Research Funds for the Central Universities of Central South University (No. 2021zzts0238).

References

[1] M.J. Gollner, X. Huang, J. Cobian, A.S. Rangwala, F.A. Williams, Experimental study of upward flame spread of an inclined fuel surface, Proc. Combust. Inst. 34 (2013) 2531-2538.

[2] Y. Huang, L. Hu, Y. Ma, N. Zhu, Y. Chen, J. Wahlqvist, M. Mcnamee, P. van Hees, Experimental study of flame spread over-thermally-thin inclined fuel surface and controlling heat transfer mechanism under concurrent wind, Int. J. Therm. Sci. 165 (2021) 106936.

[3] L. Jiang, J. He, J. Sun, Sample width and thickness effects on upward flame spread over PMMA surface, J. Hazard. Mater. 342 (2018) 114-120.

[4] Y. Pizzo, J.L. Consalvi, P. Querre, M. Coutin, B. Porterie, Width effects on the early stage of upward flame spread over PMMA slabs: Experimental observations, Fire Safety J. 44 (2009) 407-414.

[5] X. Zhu, Y. Jiang, Z. Wang, C. Xiong, Y. Xia, W. Xu, The numerical and experimental analysis of upward flame spread over the flat surface and the wavy surface, J. Hazard. Mater. 368 (2019) 644-652.

[6] J.W. Marcum, P. Rachow, P.V. Ferkul, S.L. Olson, Low pressure flame blowoff of the stagnation region of cast PMMA cylinders in axial mixed convective flow, Combust. Flame 216 (2020) 385-397.

[7] Y. Zhou, R. Bu, J. Gong, W. Yan, C. Fan, Experimental investigation on downward flame spread over rigid polyurethane and extruded polystyrene foams, Exp. Therm. Fluid Sci. 92 (2018) 346-352.

[8] W. Yan, J. Li, Y. Shen, K. Wang, Experimental investigations on the flame spread of building's vertical U-shape façade, J. Therm. Anal. Calorim. 147 (2022) 5961-5971.

[9] H. Shih, H. Wu, An experimental study of upward flame spread and interactions over multiple solid fuels, J. Fire Sci. 26 (2008) 435-453.

[10] W. An, X. Yin, M. Cai, Y. Gao, Influence of vertical channel on downward flame spread over extruded polystyrene foam, Int. J. Therm. Sci. 145 (2019) 105991.

[11] S. Tao, J. Fang, Y. Meng, H.R. Shah, L. Yang, Ignition risk analysis of common building material cylindrical PMMA exposed to an external irradiation with in-depth absorption, Constr. Build. Mater. 251 (2020) 118955.

[12] N. Liu, J. Lei, W. Gao, H. Chen, X. Xie, Combustion dynamics of large-scale wildfires, Proc. Combust. Inst. 38 (2021) 157-198.

[13] M.J. Gollner, C.H. Miller, W. Tang, A.V. Singh, The effect of flow and geometry on concurrent flame spread, Fire Saf. J. 91 (2017) 68-78.

[14] Y. Zhou, R. Bu, L. Yi, J. Sun, Heat transfer mechanism of concurrent flame spread over rigid polyurethane foam: Effect of ambient pressure and inclined angle, Int. J. Therm. Sci. 155 (2020) 106403.

[15] K. Zhao, L. Yang, W. Tang, Q. Liu, X. Ju, J. Gong, Effect of orientation on the burning and flame characteristics of PMMA slabs under different pressure environments, Appl. Therm. Eng. 156 (2019) 619-626.

[16] L. Zhao, J. Fang, X. He, J. Wang, S. Tao, Y. Zhang, An analysis of width effects on flame spread in conjunction with concurrent forced flow using a variable B-number, Combust. Flame 194 (2018) 334-342.

[17] M. Li, Y. Wang, L. Jiang, F. Gou, J. Sun, Mass loss prediction of inclined fuel combustion using variable B-number theory, Fuel 310 (2022) 122446.

[18] D.D. Drysdale, A.J.R. Macmillan, Flame spread on inclined surfaces, Fire Saf. J. 18 (1992) 245-254.

[19] Y. Zhang, J. Ji, Q. Wang, X. Huang, Q. Wang, J. Sun, Prediction of the critical condition for flame acceleration over wood surface with different sample orientations, Combust. Flame 159 (2012) 2999-3002.

[20] Y. Pizzo, J.L. Consalvi, B. Porterie, A transient pyrolysis model based on the B-number for gravity-assisted flame spread over thick PMMA slabs, Combust. Flame 156 (2009) 1856-1859.

[21] Z. Qi, H. Hu, J. Jie, Investigation on the double-sided concurrent flame spread behavior of log planks, Proc. Combust. Inst. 000 (2022) 1-10.

[22] Y. Zhou, J. Gong, L. Jiang, C. Chen, Orientation effect on upward flame propagation over rigid polyurethane foam, Int. J. Therm. Sci. 132 (2018) 86-95.

[23] P. Sun, Y. Liu, X. Huang, Exploring the brachistochrone (shortest-time) path in fire spread, Sci. Rep. 12 (2022) 13600.

[24] D. Drysdale, An introduction to fire dynamics, third edition, John Wiley & Sons, 2011.

[25] M.M. Yovanovich, On the effect of shape, aspect ratio and orientation upon natural convection from isothermal bodies of complex shape, ASME HTD 82 (1987) 121-129.

[26] C.H. Forsberg, Heat transfer principles and applications, Academic Press, 2020.

[27] L. Jiang, C.H. Miller, M.J. Gollner, J.H. Sun, Sample width and thickness effects on horizontal flame spread over a thin PMMA surface, Proc. Combust. Inst. 36 (2017) 2987-2994.

[28] Y. Ma, L. Hu, Y. Huang, N. Zhu, O. Fujita, Effect of sample thickness on concurrent stead spread behavior of floor- and ceiling flames, Combust. Flame 233 (2021) 111600.

[29] F. Jiang, J.L. de Ris, H. Qi, M.M. Khan, Radiation blockage in small scale PMMA combustion, Proc. Combust. Inst. 33 (2011) 2657-2664.

[30] A.V. Singh, M.J. Gollner, A methodology for estimation of local heat fluxes in steady laminar boundary layer diffusion flames, Combust. Flame 162 (2015) 2214-2230.